Functions of Chondroitin Sulfate/Dermatan Sulfate Chains in Brain Development: Critical Roles of E and iE Disaccharide Units Recognized by a Single Chain Antibody GD3G7*

Anurag Purushothaman[1‡], Junko Fukuda[1], Shuji Mizumoto[1,2], Gerdy B. ten Dam[3], Toin H. van Kuppevelt[3], Hiroshi Kitagawa[1], Tadahisa Mikami[1] and Kazuyuki Sugahara[1,2§]

[1]Department of Biochemistry, Kobe Pharmaceutical University, Higashinada-ku, Kobe 658-8558, Japan, [2]Laboratory of Proteoglycan Signaling and Therapeutics, Graduate School of Life Science, Hokkaido University, Frontier Research Center for Post-Genomic Science and Technology, Nishi 11-choume, Kita 21-jo, Kita-ku, Sapporo, Hokkaido 001-0021, Japan, [3]Department of Biochemistry, Radboud University Nijmegen Medical Center, 6500 HB Nijmegen, The Netherlands

Running title: Single chain antibody GD3G7 recognizing CS-E and DS-E

[§]To whom correspondence should be addressed: Laboratory of Proteoglycan Signaling and Therapeutics, Graduate School of Life Science, Hokkaido University, Frontier Research Center for Post-Genomic Science and Technology, Nishi 11-choume, Kita 21-jo, Kita-ku, Sapporo, Hokkaido 001-0021, Japan. Tel: 81-(11)-706-9054; Fax: 81-(11)-706-9056; E-mail: k-sugar@sci.hokudai.ac.jp.

Chondroitin sulfate (CS) and dermatan sulfate (DS) have been implicated in the processes of neural development in the brain. In this study, we characterized developmentally regulated brain CS/DS chains using a single chain antibody, GD3G7, produced by the phage display technique. Evaluation of the specificity of GD3G7 towards various glycosaminoglycan preparations showed that this antibody specifically reacted with squid CS-E [rich in the GlcUAβ1-3GalNAc(4,6-*O*-sulfate) disaccharide unit E], hagfish CS-H [rich in the IdoUAα1-3GalNAc(4,6-*O*-sulfate) unit iE] and shark skin DS (rich in both E and iE units). *In situ* hybridization for the expression of *N*-acetylgalactosamine-4-sulfate 6-*O*-sulfotransferase in the postnatal mouse brain, which is involved in the biosynthesis of CS/DS-E, showed a widespread expression of the transcript in the developing brain except at postnatal day 7, where strong expression was observed in the external granule cell layer in the cerebellum. The expression switched from the external to internal granule cell layer with development. Immunohistochemical localization of GD3G7 in the mouse brain showed that the epitope was relatively abundant in the cerebellum, hippocampus and olfactory bulb. GD3G7 suppressed the growth of neurites in embryonic hippocampal neurons mediated by CS-E, suggesting that the epitope is embedded in the neurite outgrowth-promoting motif of CS-E. In addition, a CS-E decasaccharide fraction was found to be the critical minimal structure needed for recognition by GD3G7. Four discrete decasaccharide epitopic sequences were identified. The antibody GD3G7 has broad applications in investigations of CS/DS chains during the central nervous system's development and under various pathological conditions.

Chondroitin sulfate (CS)[1] and dermatan sulfate (DS) chains are covalently linked to a wide range of core proteins, forming proteoglycans (PGs) with a widespread distribution in mammalian tissues (1). CS/DS-PGs are increasingly implicated as important regulators of many biological processes such as cell proliferation and recognition (2, 3), cell adhesion and migration (4-6), neurite outgrowth (6, 7), wound repair and anti-coagulation processes (8-10). CS-PGs, which constitute the major population of PGs in the central nervous system (CNS), influence the formation of neuronal nuclei and establishment of boundaries for axonal growth, and act as modulators of neuronal outgrowth (11). The CS chain's backbone consists of repetitive disaccharide units containing D-glucuronic acid (GlcUA) and *N*-acetylgalactosamine (GalNAc) residues, while DS is a sterioisomeric variant of CS with varying proportions of L-iduronic acid (IdoUA) in place of GlcUA. In mammalian tissues, these chains are often found as CS/DS hybrid structures and further structural variability of these chains during chain elongation is produced by divergent sulfation in the repeating disaccharide units by various sulfotransferases. Sulfation occurs at C-2 of GlcUA/IdoUA and/or C-4 and/or C-6 of GalNAc in various combinations, thereby producing characteristic sulfation patterns and enormous structural diversity. Recent studies have shown that proportions of these disaccharide units in chick,

mouse, and pig brain change with development (12,13), suggesting that CS/DS chains differing in the degree and profile of sulfation may be involved in the functional diversity of neurons during brain development. Moreover, oversulfated CS/DS chains from various marine animals showed growth factor-binding and neurite outgrowth-promoting activities *in vitro* (14-17).

However, the reported functions of brain CS/DS chains in neuritogenesis are controversial. CS/DS chains act as neuritogenic molecules (for reviews, see Refs. 6, 18, 19) and also as inhibitors of axonal regeneration in the injured central nervous system (20-23). Such apparently contradictory functions are probably attributed to the structural diversity of CS/DS chains. Significant and various proportions of disulfated disaccharide units such as the D unit [GlcUA(2S)-GalNAc(6S)] and E unit [GlcUA-GalNAc(4S, 6S)] are detected in the brain of cattle (24), embryonic day 13 (E13) mice (25) and E18 rats (26) (2S, 4S and 6S represent 2-*O*, 4-*O*, and 6-*O* sulfate groups, respectively). Recently, we demonstrated that the rare oversulfated disaccharide units D and/or iD [IdoUA(2S)-GalNAc(6S)] and E present in embryonic pig brain-derived CS/DS chains are critical elements for neuritogenesis (27). In addition, CS chains from appican, the amyloid precursor protein expressed by rat C6 glioma cells, contained significant proportions of D and E units (28). CS-H, isolated from the hagfish notochord, has a unique oversulfated structure characterized by a major disaccharide H (or iE) unit [IdoUA-GalNAc(4S, 6S)] (6, 18, 29, 30), and therefore is actually DS. The term DS-E for this glycosaminoglycan (GAG) and iE (where "i" stands for IdoUA) for the H disaccharide unit have been proposed (6, 18). Further, exogenous DS-E/CS-H exhibited appreciable inhibitory activity in midkine (MK)-mediated neuronal cell adhesion similar to CS-E (26). However, the presence of oversulfated CS-E and/or iE structures in the mammalian brain has not been rigorously characterized.

In biosynthesis, the structural variability of CS/DS chains is generated under the control of multiple sulfotransferases and glucuronyl C5-epimerase, which converts GlcUA to IdoUA (for reviews, see Refs. 31-33). Chondroitin 4-*O*-sulfotransferase-1 and -2 (C4ST-1 and C4ST-2) catalyze the 4-*O*-sulfation of GalNAc residues in chondroitin as well as in dermatan, while dermatan 4-*O*-sulfotransferase-1 (D4ST-1) catalyzes the 4-*O*-sulfation of GalNAc residues in dermatan (Refs. 34-37). Several other sulfotransferases like *N*-acetylgalactosamine-4-*O*-sulfotransferase-1 and –2, which catalyze 4-*O*-sulfation at the nonreducing terminal GalNAc residues in GalNAcβ1-4GlcNAcβ-, have also been cloned. On the other hand, *N*-acetylgalactosamine-4-sulfate 6-*O*-sulfotransferase (GalNAc4S-6ST), which catalyzes the transfer of sulfate to the 6-*O*-position of *N*-acetylgalactosamine-4-sulfate (GalNAc4S), has been cloned (38), but not yet analyzed in the brain. The gene expression pattern of this sulfotransferase would provide clues for investigating the distribution of CS-E chains in the brain.

Hence, we performed *in situ* hybridization to probe the distribution of GalNAc4S-6ST in postnatal mouse brain and also studied the possible functions of E/iE-containing structures in brain development using a new antibody, GD3G7, generated by the phage display technique (39). Interestingly, a good correlation between GalNAc4S-6ST expression and the GD3G7 epitope was observed in mammalian brain.

EXPERIMENTAL PROCEDURES

Materials – The ScFv antibody GD3G7 was selected for reactivity with rat embryo-derived GAGs by phage display as described by ten Dam *et al.*[2]. DNA sequence analysis revealed that antibody GD3G7 belongs to the V_H3 family, has a DP 38 germline gene segment and contains the heavy chain complementarily determining region 3 (CDR3) amino acid sequence GRWTQMT. CS-A from whale cartilage, CS-B from porcine skin, CS-C and CS-D from shark cartilage, CS-E from squid cartilage, heparin from bovine intestinal mucosa, chondroitinases ABC (EC 4.2.2.4), and AC-I (EC 4.2.2.5) and B (EC 4.2.2) were purchased from Seikagaku Corp. (Tokyo, Japan). CS-H from hagfish notochord was a gift from the late Prof. Nobuko Seno (Ochanomizu University, Tokyo, Japan) and DS from shark skin was prepared as described earlier (17). Postnatal day 7 (P7), P14, P21, 7-week-old (W) male and pregnant ddY mice were purchased from SLC Inc. (Shizuoka, Japan). The monoclonal anti-VSV tag antibody P5D4 and porcine intestinal mucosal heparin were obtained from Sigma (St. Louis, MO), and alkaline phosphatase-linked goat anti-mouse Ig (G+M) was purchased from StressGen Biotechnol Corp. (San Diego, CA). A Superdex™ Peptide HR 10/30 column was obtained from GE Healthcare Bio-Sciences (Tokyo, Japan). EZ-Link™ biotin-LC-hydrazide was obtained from Pierce (Rockford, IL). Even-numbered, saturated oligosaccharide (tetra to hexadecasaccharide) fractions were prepared by the partial enzymatic digestion of a commercial CS-E from squid cartilage with sheep testicular

hyaluronidase as described previously (40) and structurally defined CS-E octa- and decasaccharides were prepared as described by Deepa *et al*. (41). Poly-DL-ornithine (P-ORN) and anti-neurofilament antibody (NF) were purchased from Sigma, and anti-microtubule-associated protein 2 (MAP2) was from Leico Technologies Inc. (St. Louis, MO). A Vectastain ABC kit was obtained from Vector Laboratories. ^{35}S-Labeled 3'-phosphoadenosine 5'-phosphosulfate (PAPS) was purchased from PerkinElmer Life Sciences (Wellesley, MA).

Enzyme–Linked Immunosorbent Assay (ELISA) – For the evaluation of the specificity of the antibody in antigen recognition, streptavidin-coated plates were used. The reactivity of the antibody with various GAG subtypes was tested by ELISA as described previously (42). Briefly, the GAGs were individually biotinylated and immobilized on the plates. Wells were blocked with 1% bovine serum albumin (BSA) and incubated with 10-fold diluted primary antibody GD3G7. Since this antibody contains a VSV-tag, the tag was used to detect binding of the antibody. A hybridoma supernatant of the anti-VSV-tag mouse monoclonal antibody P5D4 in 0.1% BSA/PBS (diluted 5,000-fold) was used, followed by alkaline phosphatase-linked goat anti-mouse Ig (G+M). Enzymatic activity was detected using *p*-nitrophenylphosphate, and the absorbance was measured at 415 nm.

For the inhibitory ELISA, a certain amount of GAG, even-numbered oligosaccharide, or structurally defined oligosaccharide was incubated with the antibody GD3G7 (periplasmic fraction, diluted 10-fold) in a total volume of 50 µl at room temperature for 1 h before being applied to CS-E and streptavidin-coated plates. The inhibition was calculated from the reduced absorbance relative to that obtained from a control incubation without GAG.

Construction of a Soluble Form of GalNAc4S-6ST – A zebrafish GalNAc4S-6ST was identified *in silico* by a TBLASTN search using as a query sequence the mouse counterpart (GenBank™ accession NO. AB 187269). The cDNA encoding a truncated form of zebrafish GalNAc4S-6ST lacking the first NH_2-terminal 81 amino acid residues was amplified by PCR with the pGEM-T Easy Vector containing the full coding sequence of the protein using a 5'-primer containing an in-frame *Bam*HI site (5'-GCGGATCCGGGCTCTTTTTAACACC-3') and a 3'-primer containing a *Bam*HI site located 77 bp downstream from the stop codon (5'-GCGGATCCACCAAGCATCGGCC T-3'). PCR was carried out with KOD-plus-DNA polymerase (TOYOBO, Tokyo) by 30 cycles at 94 °C for 30 s, 59 °C for 42 s, and 68 °C for 90 s. The PCR products of the expected size were digested with *Bam*HI, and cloned into the *Bam*HI site of an expression vector, pEF-BOS/IP (43). The resultant vector contained the insulin leader peptide and a protein A IgG-binding domain followed by the truncated form of zebrafish GalNAc4S-6ST.

Expression of a Soluble Form of Putative GalNAc4S-6ST and Enzyme Assay–The expression plasmid was introduced into COS-1 cells in 100-mm plates using FuGENE™ 6 (Roche Applied Science) according to the manufacture's instructions. Two days after the transfection, a 1-ml aliquot of the culture medium was incubated with 10 µl of IgG-Sepharose beads (GE Healthcare Bio-Sciences) for 1 h at 4 °C. The enzyme-bound beads were washed with and resuspended in the assay buffer described below and used as an enzyme source for the sulfotransferase assay.

Sulfotransferase activity towards CS/DS was assayed by a method described previously (44). Briefly, the standard reaction mixture (60 µl) contained 10 µl of the resuspended beads, 50 mM imidazole–HCl, pH 6.8, 2 mM dithiothreitol, 10 µM [^{35}S]PAPS (1 or 3 x 10^5 dpm) and CS-B from porcine skin, which had been pretreated with nitrous acid as the acceptor polysaccharide (2 µg as GlcUA). The reaction mixture was incubated at 37 °C for 1 h and subjected to gel filtration using a syringe column packed with Sephadex G-25 (superfine) (45). The incorporation of [^{35}S]sulfate into the polysaccharide acceptor was quantified by determination of the radioactivity in the flow-through fractions by liquid scintillation counting.

Identification of the Transferase Reaction Products- The ^{35}S-labeled CS-B was isolated by gel filtration as described above, dried, and subjected to exhaustive digestion with chondroitinase ABC, AC-I, or B (46). The digest was analyzed by anion-exchange HPLC on a column of amine-bound silica PA03 (47) or by gel filtration on a column of Superdex™ Peptide (GE Healthcare Bio-Sciences) equilibrated with 0.2 M NH_4HCO_3 as described previously (48).

In situ Hybridization – Brains were quickly removed from P7, P14, P21, and 7W ddY mice and frozen in powdered dry ice. Consecutive brain sections were cut at a thickness of 16 µm with a cryostat (Leica Microsystems, Tokyo, Japan), thaw-mounted onto 3-aminopropyltriethoxysilane (APS)-precoated glass slides, and stored at –80 °C prior to use.

The pGEM-T Easy Vector containing a cDNA fragment (approximately 2.0 kbp) of mouse GalNAc4S-6ST (UniGene Cluster Mm. 213582) was linearized with a restriction enzyme, *Nco*I or *Sal*I, for synthesis of antisense or sense RNA probes, respectively. After enzymatic digestion, each digest was treated with a mixture of phenol: chloroform: isoamyl alcohol (25:24:1) and purified by ethanol precipitation. ^{35}S-Labeled riboprobes were transcribed using a MAXIscript^{TM} T7 kit (Ambion, Austin, TX) with 5'-α-[^{35}S]thiotriphosphate (approximately 30 TBq/mmol) (GE Healthcare Bio-Sciences). Before being loaded on the slides, the radiolabeled probes were mixed individually into a hybridization buffer [50% (v/v) formamide, 10% (v/v) dextran sulfate, 2.5 x Denhardt's solution, 4 x saline-sodium citrate (SSC), 5 mM EDTA, pH 8.0, 0.5 mg/ml tRNA from brewer's yeast (Roche Diagnostics, Tokyo, Japan), and 20 mM DTT] at a concentration of 10^7 cpm/ml. *In situ* hybridization was performed as described previously (49). Briefly, the brain sections were fixed in 4% (v/v) formaldehyde in phosphate-buffered saline (PBS) at room temperature for 15 min. This was followed by digestion with proteinase K (2 mg/ml) at 37 °C for 10 min, acetylation in 0.25% (v/v) acetic anhydride in 0.1M triethanolamine at room temperature for 10 min, and dehydration through graded concentrations of ethanol. After drying, the tissue sections were pretreated with the hybridization buffer without 10% (w/v) dextran sulfate at 55 °C for 1 h, then with the hybridization buffer containing the RNA probe prepared as above and incubated in a moisture chamber at 55 °C for 18 h. The sections were then rinsed twice in 2 x SSC containing 10 mM 2-mercaptoethanol (2ME) at room temperature for 5 min, digested with RNase A (50 μg/ml) at 37 °C for 30 min, rinsed twice in 50% formamide/2 x SSC/10 mM 2ME at 55 °C for 30 min and subsequently in 2 x SSC/10 mM 2ME at room temperature for 10 min, and dehydrated through graded concentrations of ethanol. The processed sections were exposed to X-ray films (Bio Max MR; Kodak, Rochester, NY) for 1 week for signal detection.

Immunohistochemistry-Immunostaining was done as described previously (27). Briefly, cryosections (18 μm thick) of mouse brain were fixed with acetone/methanol (1:1) and rehydrated with distilled water. The sections were then treated sequentially with the following solutions: 1) 2.5% hydrogen peroxidase in PBS (10 mM, pH 7.4) for 30 min; 2) 1% BSA, 4% normal horse serum in PBS for 60 min; 3) primary phage display antibody in 1% BSA/PBS (diluted 25-fold) for overnight at 4 ˚C; 4) anti-VSV tag mouse monoclonal IgG antibody, P5D4, in 1% BSA/PBS (1,000-fold) for 60 min; 5) anti-mouse IgG biotinylated antibody in 1% BSA/PBS (200-fold) for 60min; 6) Vectastain ABC solution in PBS (200-fold) for 60 min; 7) 0.06% diaminobenzidine in PBS for 10 min; 8) 0.06% diaminobenzidine, 0.01% hydrogen peroxide in PBS for 5 min. Finally, sections were fixed with a series of ethanol solutions and xylene, and then mounted with a xylene-based mounting medium. To confirm the specificity of staining with the antibody, brain sections were treated with chondroitinase ABC protease-free (5 mIU/section) to remove CS and DS. To confirm the minimal size for GD3G7, 1 nmol of the CS-E octa- or decasaccharide fraction was preincubated with the primary antibody at 37 ˚C for 60 min before being added to the sections. In this case, polyester wax sections were used as follows. Brains were fixed overnight in a 3.7% formaldehyde solution, and then dehydrated through several changes of ice-cold 70%, 90%, and absolute ethanol for 15 min at room temperature. Subsequently, brains were placed in 50% (v/v) polyester wax in absolute ethanol overnight at 37 ˚C followed by 90% polyester wax in absolute ethanol at 37 ˚C overnight. Brains were embedded in a 90% wax solution and the blocks were cut serially at 5 μm with a cryostat, and were mounted onto glass slides. The slides were dried overnight at 4 ˚C, and then processed for immunostainig as described above.

Cell Culture- Hippocampal cells were cultured using embryonic day 16.5 (E 16.5) mouse brains as described previously (16, 50). The hippocampi were obtained by microdissection and dissociated with a brief trypsin treatment. Dissociated cells were suspended in Eagle's modified essential medium containing an N2 supplement, seeded on P-ORN-coated coverslips, and cultured at 37 °C in a humidified atmosphere containing 5% CO_2.

Neurite Growth Assay- Neurite growth of hippocampal neurons from E16.5 mouse brains was assayed as described previously (16, 50). Briefly, plastic coverslips (10 x 10 mm) were treated with 1.5 μg/ml of P-ORN in 0.1 M borate buffer, pH 8.2, for 2 h at room temperature, then further coated with CS-E at a dose of 2 μg/cm^2 per coverslip in PBS at 4 °C overnight, washed with PBS three times and incubated with the antibody GD3G7 (10 and 100 μg/ml). After 2 h of incubation at room temperature, the cover slips were washed with PBS three times and then seeded with hippocampal cells at 10,000 cells/cm^2. An

irrelevant scFv antibody, MPB49V (100 μg/ml), without reactivity towards GAGs was run as a negative control.

After a 24-h culture, cells were fixed with 4% (w/v) paraformaldehyde and then immunostained with anti-MAP2 and anti-neurofilament antibodies. The antibodies were detected using a Vectastain ABC kit with DAB as a chromagen as described above. Neurite outgrowth was evaluated by determining the total length of neurites per cell. One hundred clearly isolated cells with at least one neurite longer than the cell body were chosen at random per coverslip. The results were expressed as the mean ± S.E., and the significance of differences between means was evaluated with Student's t test.

RESULTS

Evaluation of the Specificity of Antibody GD3G7 by ELISA

The reactivity of GD3G7 towards various GAG preparations was tested using ELISA, in which biotinylated GAGs were individually immobilized onto streptavidin-coated plates. GD3G7 specifically reacted with CS-E, CS-H (oversulfated DS from hagfish notochord, which contains iE as the predominant disaccharide unit) and also with SS-DS (DS from shark skin, which contains an appreciable proportion of E and iE units) and not with any other GAGs tested including CS-A, CS-B, CS-C, CS-D and heparin (Fig. 1). It should be emphasized that GD3G7 could recognize both E [GlcUA-GalNAc(4S, 6S)] and iE [IdoUA-GalNAc(4S, 6S)] units. To further investigate the specificity of GD3G7 toward iE, an inhibitory ELISA was performed, in which CS-B treated for enzymatic sulfation with or without GalNAc4S-6ST was used as the inhibitor.

Human GalNAc4S-6ST transfers sulfate from PAPS to the C-6 hydroxyl group of the GalNAc-4-*O*-sulfate residues of CS-A and DS to form GlcA-GalNAc(4S, 6S) and/or IdoUA-GalNAc(4S, 6S) units (38). To facilitate the functional analysis of GalNAc4S-6ST, the activity of a zebrafish counterpart was assayed using CS-B as the acceptor and PAPS as the donor substrate. To identify the reaction products, first gel filtration was conducted using a Sephadex G-25 (superfine) column and then an aliquot of the flow-through fraction was digested exhaustively with chondroitinase ABC, chondroitinase AC-I, or chondroitinase B. It should be noted that the sulfation of GalNAc residues flanking a target IdoUA residue is essential for the action of chondroitinase B (46), although chondroitinase AC-I reactions are little influenced by the sulfation pattern of neighboring sugar residues. One half of each digest was analyzed by gel filtration on a Superdex^{TM} Peptide column (Fig. 2A-C) and the other half of each digest was analyzed by anion-exchange HPLC on an amine-bound silica PA-03 column using a linear NaH_2PO_4 gradient from 16 to 530 mM over a 1 h period (Fig. 2D-F).

The gel filtration chromatograms revealed that the ^{35}S-labeled products after digestion with chondroitinase ABC or B eluted at the position corresponding to disaccharides (Fig. 2A, C) while no detectable disaccharide products were eluted after digestion with chondroitinase AC-I (Fig. 2B). The integrated radioactivity of the disaccharide peak observed on gel filtration was well consistent with that of ΔDi-diS_E (ΔE) detected by anion-exchange HPLC analysis using the other half of each digest, demonstrating that the majority of ^{35}S-labeled ΔDi-diS_E was released from the -IdoUA-GalNAc(4S, 6S)-IdoUA- sequence by digestion with chondroitinase ABC and chondroitinase B (Fig. 2D, F) and not from the -GlcUA-GalNAc(4S, 6S)-GlcUA- sequence, since no products were detected after treatment with chondroitinase AC-I (Fig. 2E). These results suggest that when CS-B was used as the acceptor molecule, GalNAc4S-6ST catalyzed the sulfation of GalNAc(4S) residues adjacent to IdoUA rather than GlcUA, thereby generating iE disaccharide units. Under the same assay condition, a soluble form of mouse GalNAc4S-6ST also catalyzed the formation of iE units, although only a relatively small proportion (29%) of the total radioactivity was detected at the position of ΔE for the chondroitinase B digest (data not shown). Hence, to produce iE units *in vitro*, the soluble form of zebrafish GalNAc4S-6ST was used for enzymatic synthesis of iE unit-containing polysaccharides as described below.

Evaluation of Specificity of GD3G7 towards iE

Zebrafish GalNAc4S-6ST preferentially transferred sulfate to the 6-*O*-position of GalNAc(4S) residues adjacent to IdoUA residues in CS-B, which contains approximately 95% IdoUA-GalNAc(4S), thereby generating iE [IdoUA-GalNAc(4S, 6S)] disaccharide units. To further evaluate the specificity of GD3G7 towards iE, we assessed the ability of CS-B treated with or without GalNAc4S-6ST to inhibit the binding of GD3G7 to immobilized CS-E. As shown in Fig. 3, CS-B treated with GalNAc4S-6ST showed significant inhibition for the binding of GD3G7 to CS-E, while CS-B not treated with GalNAc4S-6ST showed no inhibition against the binding of

GD3G7 to CS-E, suggesting that GD3G7 specifically reacted with iE. Inhibitory activity was also exhibited by CS-H but not CS-D. The current data thus support the conclusion that GD3G7 recognizes both E and iE disaccharide units.

Expression of GalNAc-4-Sulfate 6-O-Sulfotransferase in the Mouse Brain During Postnatal Development

CS/DS chains regulate the development of the central nervous system and play various roles as neuritogenic molecules. It has been previously demonstrated that IdoUA- containing structures in CS/DS hybrid chains from embryonic pig brain are essential for neuritogenic and growth factor-binding activity (51). Hence, to gain insights into the distribution of CS/DS hybrid chains containing E/iE units in the mouse brain during postnatal development, expression of the mouse GalNAc4S-6ST was examined by *in situ* hybridization with the ^{35}S-labeled antisense probe.

Fig. 4 presents film-autoradiograms of sagittal sections from the brains of P7 (Fig. 4A), P14 (Fig. 4B) and P21 (Fig. 4C) mice. The GalNAc4S-6ST transcript was observed in many regions of the developing brain including the olfactory bulb, cerebral cortex, hippocampus, cerebellum and striatum. In a negative control experiment with the ^{35}S-labeled sense probe, no labeling was observed in any region of brain sections of a P21 mouse (Fig. 4E) or in a P7 or P14 mouse (data not shown), confirming the specific hybridization of the antisense probe. The expression of this gene was confined to the cerebellum in P7 mice, with strong expression observed in the external granule cell layer (Fig. 4A). The cerebellar expression switched from the external granule cell layer to internal granule cell layer, and appeared to decrease slightly with development (Fig. 4A-D), probably reflecting the migration and/or maturation of granular cells. This gene expression suggests that CS/DS chains containing E and/or iE units are relatively abundant in the cerebellum of P7 mice and gradually decrease during postnatal development. It is interesting to note that GalNAc4S-6ST message was also highly expressed in the dentate gyrus of hippocampus and olfactory bulb (Fig. 4A-D), where neurons are continuously replaced throughout life (52), and in the striatum (Fig. 4A-D). The gene expression profile provides insight into the possible involvement of the E/iE unit-containing CS/DS chains in neurogenesis and in the organization of the nigrostriatal system.

Immunohistochemical Detection and Distribution of GD3G7 Epitope in the Mouse Brain

To study the expression of the unique GD3G7 epitope in the mouse brain, immunohistochemical expression of P7 brain sections was performed using the antibody GD3G7. Consecutive sagittal sections from P7 mouse brain were incubated with GD3G7 and the bound antibodies were detected by anti-VSV-tag P5D4 antibodies and biotinylated anti-mouse IgG antibodies tagged with peroxidase, and visualized by DAB (the substrate for peroxidase). The staining pattern of the sagittal sections of P7 mice is shown in Fig. 5. GD3G7 specifically stained the P7 cerebellum, hippocampus and olfactory bulb. The staining was stronger in the cerebellum, where GD3G7 stained most intensely the developing molecular layer at its border with external granular layer. During the neonatal development of the cerebellum, the generation of granule cells occurs in the proliferative zone of the external granular layer (53), where GalNAc4S-6ST was strongly expressed (Fig. 4A). Granule cells start to exit the cell cycle after birth and as part of their differentiation program they migrate internally, passing through the molecular layer and Purkinje cells to form the inner granular layer (54). Since the staining of the molecular layer was reduced in the P21 sections (data not shown), the staining of the molecular layer with GD3G7 at P7 may be, in part, due to the close apposition of internally migrating granule cells. In the hippocampus, the GD3G7 reactivity was observed in the areas surrounding the pyramidal cell layer of the CA1-CA3 fields and the granular cell layer of the dentate gyrus, In the olfactory bulb, the GD3G7 epitope was expressed in the glomerular layer as well as the external and plexiform layers. These staining patterns in the hippocampus and olfactory bulb are indicative of a role for the epitope in axon tract formation. The staining of the brain was completely abolished on the treatment of the tissue sections with chondroitinase ABC, confirming the specificity of the staining. These results suggest that CS-E is highly expressed in the cerebellum and also in the hippocampus and olfactory bulb of P7 mouse brain.

Effects of GD3G7 on the Neurite Outgrowth of Hippocampal Neurons

CS-E promotes the outgrowth of neurites in rat E18 hippocampal neurons. The antibody GD3G7 recognizes an epitope structure embedded in CS-E. To investigate whether the GD3G7 epitope in CS-E is involved in the process of neurite outgrowth in hippocampal neurons, the antibody was added to

the culture medium at two different concentrations (10 μg/ml and 100 μg/ml) 2 h prior to the seeding of the neuronal cells on the substratum coated with CS-E. The antibody significantly suppressed the growth of neurites in the neurons grown on the substratum containing CS-E (Fig. 6A and B). This observation was confirmed by a statistical morphometric analysis, which revealed that GD3G7 markedly inhibited the formation of neurites and decreased the total length of neurites per cell at a concentration of 100 μg/ml (Fig. 6C). These results demonstrated that the epitope of GD3G7 is embedded in the neurite outgrowth-promoting motif of CS-E. Control scFv antibody (MPB49V, 100 μg/ml) showed no neutralizing activity.

Characterization of the Minimal Structure Required for Recognition by GD3G7

In view of the finding that the epitope of GD3G7 in CS-E may be involved in the neurite outgrowth-promoting activity, we characterized the minimal structure of CS-E required for recognition by this antibody. Even-numbered CS-E oligosaccharide fractions, which were prepared by partial digestion of CS-E from squid cartilage with sheep testicular hyaluronidase (40), were used as inhibitors for the binding of GD3G7 to immobilized CS-E. Fig. 7A shows that deca- and larger oligosaccharides exhibited inhibitory activity, and the activity increased with molecular size, although the octasaccharide fraction seemed to react only slightly with GD3G7 compared with the hexasaccharide fraction.

Next, to precisely determine the minimal structure of CS-E recognized by GD3G7, varying doses of CS-E octa- and decasaccharides were used as inhibitors against the binding of GD3G7 to CS-E. Fig. 7B shows that GD3G7 reacted preferentially with the decasaccharide fraction from CS-E but not at all with the octasaccharide fraction. The degree of binding of GD3G7 to the CS-E decasaccharide fraction increased in a dose-dependent manner, whereas there was no binding to the octasaccharide fraction even at higher doses. These results were consistent with the above finding that the decasaccharide fraction derived from CS-E meets the critical minimal size needed for recognition by GD3G7.

We sought to corroborate the ELISA data by assessing the immunoreactivity of the antibody in brain sections using CS-E oligosaccharides as inhibitors. CS-E derived octa- and decasaccharide fractions were used as inhibitors for the immunohistochemical staining of mouse brain sections from postnatal day 7. GD3G7 was incubated with 1 nmol each of the CS-E octa- and decasaccharide fractions at room temperature for 1 h prior to the incubation with the brain sections. The staining pattern of the sagittal sections from the brain of P7 mice is shown in Fig. 8. Preincubation of GD3G7 with the CS-E decasaccharide prevented the antibody from staining the sections whereas immunostaining in the cerebellum, hippocampus and olfactory bulb was still visible, when the CS-E octasaccharide was used as an inhibitor. The finding that the CS-E decasaccharide fraction was the most efficient inhibitor of GD3G7 indicates that a CS-E-derived decasaccharide fraction is the minimal structural requirement for the binding of GD3G7.

To further characterize the epitope structure of GD3G7, four structurally defined decasaccharide fractions and one octasaccharide fraction derived from CS-E were used in an inhibitory ELISA experiment for the binding of GD3G7 to CS-E. It was found that all the four decasaccharide fractions inhibited the binding of GD3G7 to immobilized CS-E but the octasaccharide fraction did not (Fig. 9), which is basically in agreement with the size-dependent reactivities observed in Fig. 7B. The structure of the oligosaccharides is summarized in Table I. GD3G7 reacted preferentially with all the structurally defined decasaccharides, whereas the octasaccharide with four E units was not bound by this antibody. The observed binding preference suggests that this antibody can recognize decasaccharides with a minimum of three consecutive E units.

DISCUSSION

In this study, the characteristic spatiotemporal distribution of CS-E/DS-E hybrid chains in the postnatal mouse brain was examined in detail using an antibody, GD3G7, produced by the phage display technique. This antibody reacted specifically with CS-E, but also with CS-H, which consists of characteristic iE units (29, 30, 55) and with SS-DS, where E (or iE) units account for 10% of all the disaccharide (17), as evaluated by ELISA, suggesting that the essential recognition unit is a GalNAc(4S, 6S) residue irrespective of whether GlcUA or IdoUA is attached to it. CS-H is derived from the hagfish notochord (29), and the corresponding mammalian tissue produces the soluble Sonic Hedgehog protein, implicated in the generation of ventral neurons and the differentiation of motor neurons (56). CS-H is structurally similar to CS-E, but contains IdoUA instead of GlcUA as a major uronic acid, and is regarded as an oversulfated DS (26). *In situ* hybridization for GalNAc4S-6ST, which is involved in the biosynthesis of CS-E/DS-E,

showed that CS-E/DS-E hybrid chains are more concentrated in the cerebellum, providing insight into the importance of these hybrid chains during the brain's development. GalNAc4S-6ST transfers sulfate from PAPS to position 6 of GalNAc(4S) in CS and DS (38). *In vitro* synthesis of DS-E from CS-B was carried out using purified GalNAc4S-6ST, which preferentially generated IdoUAα1-3GalNAc(4S,6S). Interestingly, the product inhibited the binding of GD3G7 to immobilized CS-E, indicating that the antibody GD3G7 recognized an iE-enriched region in CS-B. Thus, GD3G7 recognizes both E and iE units and will be a useful tool to study the distribution of E- and iE-containing CS/DS structures.

The importance of the differential expression of sulfotransferases has not been fully evaluated. Kitagawa *et al.* (13) demonstrated that the sulfation profile of CS chains and the ratio of the sulfotransferase C4ST and chondroitin 6-*O*-sulfotransferase (C6ST) activities forming the specific sulfation profile changed markedly with development in the chick embryonic brain, and these alterations were precisely coordinated. Here, we have shown for the first time the distribution of *GalNAc4S-6ST* in the developing brain. The strong expression of *GalNAc4S-6ST* was confined in the external granule cell layer in the cerebellum (Fig. 4A) of P7 mouse brain. Its restricted expression switched to the internal granule cell layer and probably the Purkinje cell layer, and decreased slightly with development, demonstrating that E/iE-containing CS/DS chains play critical roles during brain development. *GalNAc4S-6ST* was also found to be strongly expressed in the olfactory bulb, hippocampus, cerebral cortex and striatum of the developing brain, suggesting the involvement of E/iE-containing CS/DS chains in neurogenesis, axon guidance, and/or neuronal survival in these regions. Recently, it has been demonstrated that appican, the CS-PG form of the Alzheimer's amyloid precursor protein, produced by glioma cells, contains 14.3% CS-E (28). The CS chain in appican is responsible for the adhesion of neural cells and for promoting the outgrowth of neurites in primary rat hippocampal cultures, because the core of the Alzheimer's amyloid precursor protein is less potent in promoting adhesion and neurite outgrowth than is appican PG (57, 58). The presence of E units in appican PG may explain the neurotrophic activities of appican. The hypothesis that oversulfated disaccharides are mainly responsible for the neurotrophic activities shown by specific CS-PGs is based on the pioneering observations that oversulfated squid CS-E as well as shark CS-D promotes neurite outgrowth in cultures of primary rat hippocampal neurons (15, 59). By contrast, CS-PGs lacking oversulfated units either fail to promote neurite outgrowth or show inhibitory activity (60). Our observation that the postnatal brain contains oversulfated E units supports this hypothesis and suggests that CS-E/DS-E may function in the brain to promote neurite outgrowth. Recently, it has been demonstrated that CS-E can bind various growth factors (61), suggesting that its neuroregulatory activities are exerted through signal transduction mediated by various growth factors. In fact, it was recently demonstrated that CS/DS chains derived from embryonic pig brain recruited endogenous PTN to promote neuritogenesis in a hippocampal cell culture system (42), although the core proteins of the CS/DS chains have not been identified. Previously, a transmembrane PG, syndecan-1 from mouse mammary gland epithelial cells, was demonstrated to bear E-containing CS chains (62), although it is unknown whether syndecan-1, expressed in the rat central nervous system, which binds MK and PTN (63), contains CS-E.

The E unit has been demonstrated in appreciable proportions in CS chains from bovine brain (24) and chick brain, where it exhibits a developmentally regulated expression (13). Interestingly, the antibody GD3G7 stained restricted regions in the P7 mouse brain, indicating the expression of CS-E/DS-E-containing structures in the mammalian brain. However, it remains to be determined whether the GD3G7 epitope in the mouse brain is embedded in the DS domains that contain iE units. Oversulfated disaccharides such as D/iD, B/iB, and E/iE have been implicated in the development of the brain (6, 16, 18). Recently, Bao *et al.* (27) demonstrated the presence of functional iD-containing domains in the developing mouse brain using a monoclonal antibody, 2A12, against the DS from ascidian. Maeda *et al.* (12) have reported the systematic immunohistochemical localization of several CS epitopes, including CS-56 and MO-225 epitopes in the developing postnatal mouse brain. The CS-56 epitope is highly expressed in the cerebral cortex early in the postnatal period, and its expression is markedly decreased three weeks after birth (12). In contrast, the expression of the MO-225 epitope is weak in the cerebral cortex but stronger in other regions, including the cerebellum, during the developing stages. MO-225 reactivity in the cerebellum reaches a peak at postnatal day 14 and decreases thereafter (12). The original study by Yamagata *et al.* (64) showed the reactivity of MO-225 with the tetrasaccharides ΔA-D and ΔE-D. Recently, Ito *et al*. (65) have shown that MO-225 could

strongly react with octa- and larger oligosaccharide fractions derived from CS-D of shark cartilage, and Deepa *et al.*[3] showed that MO-225 reacted with a decasaccharide sequence rich in E units, prepared from squid cartilage CS-E.

CS-E promoted the outgrowth of axon-like neurities toward neurons in a hippocampal cell culture (15). GD3G7 antibody inhibited the neuritogenic activity mediated by CS-E, suggesting that the functional domain for the neuritogenic activity of the CS-E chains also includes the GD3G7 epitope. Ueoka *et al.* (26) have shown the presence of CS-E in E18 rat brains and also that the oversulfated E motif appears to be involved in the neuroregulatory activities of MK. It remains to be investigated, however, which CS-PGs in the brain contain the E motif. Despite the identification of soluble CS-PGs such as brevican (66) and neurocan (67) as well as transmembrane CS-PGs such as NG2 (68), PTPζ and neuroglycan C (69), the CS chains attached to the core proteins have not been rigorously investigated. Maurel *et al.* (70) have shown that phosphacan, an extracellular variant of PTPζ, a receptor-type protein tyrosine phosphatase that is abundantly expressed in the brain, binds PTN, which binds to the same gene family as MK, and the binding of PTN to phosphacan/PTPζ was dependent on the CS portion of this proteoglycan, and various CS preparations competitively inhibited this binding (71, 72). Notably, squid cartilage CS-E, which has a high proportion of E units, inhibited the binding very efficiently, suggesting that oversulfated CS structures play important roles in the binding of phosphacan/PTPζ to PTN (71, 72). It is possible that PTPζ and/or phosphacan bear CS chains with distinctive sulfation profiles during different developmental stages. PTPζ/phosphacan-PTN signaling is involved in the neurite extension, neuronal migration, glioma migration, and morphogenesis of Purkinje cells (for reviews, see Ref. 71-75). Deepa *et al.* (61) have shown that PTN and MK interact with CS-E. In view of these reports, the possibility cannot be excluded that specific oligosaccharide sequences in the brain containing E/iE units are responsible for the high-affinity binding of MK and PTN to PTPζ and thereby mediating the neuritogenesis of cerebellar neurons.

We also demonstrated that a CS-E decasaccharide fraction was the smallest oligosaccharide fraction to inhibit the binding of GD3G7 to CS-E and larger oligosaccharide fractions showed stronger inhibition. The CS-E decasaccharide fraction also had an inhibitory effect on the reactivity of GD3G7 with sections of mouse brain, confirming the notion that the decasaccharide was the minimal size required for the binding of GD3G7. The reactivity of GD3G7 with structurally defined octa- and decasaccharides suggests that a decasaccharide with three consecutive E units may be a possible epitope structure for GD3G7 but not an octasaccharide with four consecutive E units. Thus, it was concluded that not only the E units but also size is important for recognition by this antibody. Also, the possibility cannot be excluded that the GD3G7 epitope in the brain may be a decasaccharide with core E- and or iE-units or a mixture of E/iE-units scattered along the functional domain. The isolation of GD3G7-reactive structures from brain-derived CS/DS chains will help clarify the structures of this unique epitope.

The results altogether demonstrate that CS-E/DS-E expressed in the brain plays vital roles during brain development. The human scFv antibody described here can be used as a tool to visualize structural diversity in CS as illustrated for other antibodies (76, 77). Since the cDNA of the single chain antibody is available, antibodies can be produced and purified in large quantities. It will be interesting to identify the PGs carrying such a unique E/iE-containing GD3G7 epitope, which would provide valuable information on the functions of CS-PGs during the development of the central nervous system.

Acknowledgments-We thank Noriyo Kaide for preparation of even-numbered oligosaccharides from CS-E, and Sarama Sathyaseelan Deepa, Kittiwan Kalayanamitra, and Yumi Ito for the preparation of structurally defined CS-E octa- and decasaccharides.

REFERENCES

1. Rosenberg, L. C., Choi, H. U., Tang, L. H., Johnson, T. L., Pal, S., Webber, C., Reiner, A., and Poole, A. R. (1985) *J. Biol. Chem.* **260**, 6304-6313
2. Yamaguchi, Y., Mann, D. M., and Ruoslahti, E. (1990) *Nature* **346**, 281-284
3. Lyon, M., Deakin, J. A., Rahmoune, H., Fernig, D. G., Nakamura, T., and Gallagher, J. T. (1998) *J. Biol. Chem.* **273**, 271-278

4. Schwartz, N. B., and Domowicz, M. (2002) *Glycobiology* **12**, 57R-68R
5. Kinsella, M. G., Tsoi, C. K., Jarvelainen, H. T., and Wight, T. N. (1997) *J. Biol. Chem.* **272**, 318-325
6. Sugahara, K., Mikami, T., Uyama, T., Mizuguchi, S., Nomura, K., and Kitagawa, H. (2003) *Curr. Opin. Struct. Biol.* **13**, 612-620
7. Lafont, F., Rouget, M., Triller, A., Prochiantz, A., and Rousselet, A. (1992) *Development* **114**, 17-29
8. Penc, S. F., Pomahac, B., Winkler, T., Dorschner, R. A., Eriksson, E., Herndon, M., and Gallo, R. L. (1998) *J. Biol. Chem.* **273**, 28116-28121
9. Liaw, P. C., Becker, D. L., Stafford, A. R., Fredenburgh, J. C., and Weitz, J. I. (2001) *J. Biol. Chem.* **276,** 5228-5234
10. Trowbridge, J. M., Rudisill, J. A., Ron, D., and Gallo, R. L. (2002) *J. Biol. Chem.* **277**, 42815-42820
11. Schwartz, N. B., and Domowicz, M. (2004) *Glycoconj. J.* **21**, 329-341
12. Maeda, N., He, J., Yajima, Y., Mikami, T., Sugahara, K., and Yabe, T. (2003) *J. Biol. Chem.* **278**, 35805-35811
13. Kitagawa, H., Tsutsumi, K., Tone, Y., and Sugahara, K. (1997) *J. Biol. Chem.* **272**, 31377-31381
14. Nadanaka, S., Clement, A., Masayama, K., Faissner, A., and Sugahara, K. (1998) *J. Biol. Chem.* **273**, 3296-3307
15. Clement, A., Sugahara, K., and Faissner, A. (1999) *Neurosci. Lett.* **269**, 125-128
16. Hikino, M., Mikami, T., Faissner, A., Vilela-Silva, A. C., Pavao, M. S., and Sugahara, K. (2003) *J. Biol. Chem.* **278**, 43744-43754
17. Nandini, C. D., Itoh, N., and Sugahara, K. (2005) *J. Biol. Chem.* **280**, 4058-4069
18. Sugahara, K., and Yamada, S. (2000) *Trends Glycosci. Glycotechnol.* **12**, 321-349
19. Bandtlow, C. E., and Zimmermann, D. R. (2000) *Physiol. Rev.* **80**, 1267-1290
20. Moon, L. D., Asher, R. A., Rhodes, K. E., and Fawcett, J. W. (2001) *Nat. Neurosci.* **4**, 465-466
21. Bradbury, E. J., Moon, L. D., Popat, R. J., King, V. R., Bennett, G. S., Patel, P. N., Fawcett, J. W., and McMahon, S. B. (2002) *Nature* **416**, 636-640
22. Rhodes, K. E., and Fawcett, J. W. (2004) *J. Anat.* **204**, 33-48
23. Silver, J., and Miller, J. H. (2004) *Nat. Rev. Neurosci.* **5**, 146-156
24. Saigo, K., and Egami, F. (1970) *J. Neurochem.* **17**, 633-647
25. Zou, P., Zou, K., Muramatsu, H., Ichihara-Tanaka, K., Habuchi, O., Ohtake, S., Ikematsu, S., Sakuma, S., and Muramatsu, T. (2003) *Glycobiology* **13,** 35-42
26. Ueoka, C., Kaneda, N., Okazaki, I., Nadanaka, S., Muramatsu, T., and Sugahara, K. (2000) *J. Biol. Chem.* **275,** 37407-37413
27. Bao, X., Pavao, M. S., Dos Santos, J. C., and Sugahara, K. (2005) *J. Biol. Chem.* **280**, 23184-23193
28. Tsuchida, K., Shioi, J., Yamada, S., Boghosian, G., Wu, A., Cai, H., Sugahara, K., and Robakis, N. K. (2001) *J. Biol. Chem.* **276,** 37155-37160
29. Anno, K., Seno, N., Mathews, M. B., Yamagata, T., and Suzuki, S. (1971) *Biochem. Biophys. Acta* **237,** 173-177
30. Ueoka, C., Nadanaka, S., Seno, N., Khoo, K. H., and Sugahara, K. (1999) *Glycoconj. J.* **16,** 291-305
31. Fransson, L. A., Belting, M., Jonsson, M., Mani, K., Moses, J., and Oldberg, A. (2000) *Matrix Biol.* **19,** 367-376
32. Habuchi, O. (2000) *Biochem. Biophys. Acta* **1474,** 115-127
33. Silbert, J. E., and Sugumaran, G. (2002) *IUBMB Life* **54,** 177-186
34. Mikami, T., Mizumoto, S., Kago, N., Kitagawa, H., and Sugahara, K. (2003) *J. Biol. Chem.* **278**, 36115-36127
35. Yamauchi, S., Mita, S., Matsubara, T., Fukuta, M., Habuchi, H., Kimata, K., and Habuchi, O. (2000) *J. Biol. Chem.* **275,** 8975-8981
36. Hiraoka, N., Nakagawa, H., Ong, E., Akama, T. O., Fukuda, M. N., and Fukuda, M. (2000) *J. Biol. Chem.* **275,** 20188-20196
37. Okuda, T., Mita, S., Yamauchi, S., Matsubara, T., Yagi, F., Yamamori, D., Fukuta, M., Kuroiwa, A., Matsuda, Y., and Habuchi, O. (2000) *J. Biochem. (Tokyo)* **128,** 763-770
38. Ito, Y., and Habuchi, O. (2000) *J. Biol. Chem.* **275**, 34728-34736
39. Smetsers, T. F., van de Westerlo, E. M., ten Dam, G.B., Overes I. M., Schalkwijk, J., van Muijen, G. N., and van Kuppevelt, T. H. (2004) *J. Invest. Dermatol.* 122, 707-716

40. Kinoshita, A., Yamada, S., Haslam, S. M., Morris, H. R., Dell, A., and Sugahara, K. (1997) *J. Biol. Chem*. **272**, 19656-19665
41. Deepa, S. S., Kalayanamitra, K., Yumi Ito, Kongtaweelert, P., Fukui, S., Yamada, S., Mikami, T., and Sugahara, K. *Biochemistry*, in press
42. Bao, X., Mikami, T., Yamada, S., Faissner, A., Muramatsu, T., and Sugahara, K. (2005) *J. Biol. Chem*. **280**, 9180-9191
43. Kitagawa, H., Egusa, N., Tamura, J., Kusche-Gullberg, M., Lindahl, U., and Sugahara, K. (2001) *J. Biol. Chem.* **276,** 4834-4838
44. Yamauchi, S., Hirahara, Y., Usui, H., Takeda, Y., Hoshino, M., Fukuta, M., Kimura, J. H., and Habuchi, O. (1999) *J. Biol. Chem.* **274,** 2456-2463
45. Kitagawa, H., Tsuchida, K., Ujikawa, M., and Sugahara, K. (1995) *J. Biochem. (Tokyo)* **117,** 1083-1087
46. Sugahara, K., Ohkita, Y., Shibata, Y., Yoshida, K., and Ikegami, A. (1995) *J. Biol. Chem.* **270,** 7204-7212
47. Sugahara, K., Okumura, Y., and Yamashina, I. (1989) *Biochem. Biophys. Res. Commun.* **162,** 189-197
48. Kim, B.T., Kitagawa, H., Tamura, J., Saito, T., Kusche-Gullberg, M., Lindahl, U., and Sugahara, K. (2001) *Proc. Natl. Acad. Sci. USA* **98,** 7176-7181
49. Simmons, D. M., Arriza, J. L., and Swanson, L. W. (1989) *J. Histotech*. **12**, 169-181
50. Faissner, A., Clement, A., Lochter, A., Streit, A., Schutte, K., Mandl, C., and Schachner, M. (1994) *J. Cell Biol*. **126**, 783-799
51. Bao, X., Nishimura, S., Mikami, T., Yamada, S., Itoh, N., and Sugahara, K. (2004) *J. Biol. Chem*. **79**, 9765-9776
52. Lledo, P. M., Alonso, M., and Grubb, M. S. (2006) *Nat. Rev. Neurosci.* **7**, 179-193
53. Altman, J. (1972) *J. Comps. Neurol*. **145**, 353-398
54. Wang, V. Y., and Zoghbi, H. Y**.** (2001) *Nat. Rev. Neurosci.* **2**, 484 –491
55. Nandini, C. D., Mikami, T., Ohta, M., Itoh, N., Akiyama-Nambu, F., and Sugahara, K. (2004) *J. Biol. Chem.* **279**, 50799-50809
56. Pons, S., and Marti, E. (2000) *Development* **127**, 333-342
57. Salinero, O., Moreno-Flores, M. T., and Wandosell, F. (2000) *J. Neurosci. Res.* **60**, 87-97
58. Wu, A., Pangalos, M. N., Efthimiopoulos, S., Shioi, J., and Robakis, N. K. (1997) *J. Neurosci.* **17**, 4987-4993
59. Clement, A. M., Nadanaka, S., Masayama, K., Mandl, C., Sugahara, K., and Faissner, A. (1998) *J. Biol. Chem.* **273,** 28444-28453
60. Properzi, F., Carulli, D., Asher, R. A.,Muir, E., Camargo, L. M., van Kuppevelt, T. H., ten Dam, G. B., Furukawa, Y., Mikami, T., Sugahara, K., Toida, T., Geller, H. M., and Fawcett, J. W. (2005) *Eur. J. Neurosci*. **21**,378-390
61. Deepa, S. S., Umehara, Y., Higashiyama, S., Itoh, N., and Sugahara, K. (2002) *J. Biol. Chem*. **277**, 43707-43716
62. Ueno, M., Yamada, S., Zako, M., Bernfield, M., and Sugahara, K. (2001) *J. Biol. Chem.* **276**, 29134-29140
63. Nakanishi, T., Kadomatsu, K., Okamoto, T., Ichihara-Tanaka, K., Kojima, T., Saito, H., Tomoda, Y., and Muramatsu, T. (1997) *J. Biochem.* (*Tokyo*) **121**, 197-205
64. Yamagata, M., Kimata, K., Oike, Y., Tani, K., Maeda, N., Yoshida, K., Shimomura, Y., Yoneda, M., and Suzuki, S. (1987) *J. Biol. Chem.* **262**, 4146-4152
65. Ito, Y., Hikino, M., Yajima, Y., Mikami, T., Sirko, S., von Holst, A., Faissner, A., Fukui, S., and Sugahara, K. (2005) *Glycobiology* **15**, 593-603
66. Yamada, H., Watanabe, K., Shimonaka, M., and Yamaguchi, Y. (1994) *J. Biol. Chem.* **269**, 10119-10126
67. Engel, M., Maurel, P., Margolis, R. U., and Margolis, R. K. (1996) *J. Comp. Neurol.* **366**, 34-43
68. Stallcup, W. B. (1981) *Dev. Biol.* **83**, 154-165
69. Watanabe, E., Maeda, N., Matsui, F., Kushima, Y., Noda, M., and Oohira, A. (1995) *J. Biol. Chem.* **270**, 26876-26882
70. Maurel, P., Rauch, U., Flad, M., Margolis, R. K., and Margolis, R. U. (1994) *Proc. Natl. Acad. Sci. USA* **91**, 2512-2516
71. Maeda, N., Nishiwaki, T., Shintani, T., Hamanaka, H., and Noda M. (1996) *J. Biol. Chem.* **271**, 21446-21452

72. Maeda, N., Ichihara-Tanaka, K., Kimura, T., Kadomatsu, K., Muramatsu, T., and Noda, M. (1999) *J. Biol. Chem.* **274**, 12474-12479
73. Maeda, N., and Noda, M. (1998) *J. Cell Biol*. **142**, 203-216
74. Muller, S., Kunkel, P., Lamszus, K., Ulbricht, U., Lorente, G. A., Nelson, A.M., Schack, D., Chin, D.J., Lohr, S. C., Westphal, M., and Melcher, T. (2003) *Oncogene* **22**, 6661-6668
75. Tanaka, M., Maeda, N., Noda, M., and Marunouchi, T. (2003) *J.Neurosci.* **23**, 2804-2814
76. Sorrell, J. M., Carrino, D. A., and Caplan, A. I. (1993) *Matrix* **13**, 351-361
77. Sorrell, J. M., Carrino, D. A., Baber, M. A., Asselineau, D., and Caplan, A. I. (1999) *Histochem. J*. **31**, 549-558

FOOTNOTES

*****The work performed in Kobe was supported in part by the Scientific Research Promotion Fund from the Japan Private School Promotion Foundation, Grants-in-aid #17659020, #18390030, #14082207 and Encouragement of Young Scientists 118790073 (to T. M.) from MEXT, the Human Frontier Science Program, the Core Research for Evolutional Science and Technology (CREST) program of the Japan Science and Technology (JST) Agency. The work in Nijmegen was supported by the Dutch Cancer Society, grant number 2002-2762 (to G.t.D.).

‡ Supported by a postdoctoral fellowship of HAITEKU (2004 – 2005) from the Japan Private School Promotion Foundation.

[1]The abbreviations used in this paper are: CS, chondroitin sulfate; DS, dermatan sulfate; GAG, glycosaminoglycan; PG, proteoglycan; GlcUA, D-glucuronic acid; GalNAc, *N*-acetylgalactosamine; IdoUA, L-iduronic acid; 2S, 2-*O*-sulfate; 4S, 4-*O*-sulfate; 6S, 6-*O*-sulfate; MK, midkine; C4ST, chondroitin-4-*O*-sulfotransferase; D4ST, dermatan-4-*O*-sulfotransferase; GalNAc4S-6ST, *N*-acetylgalactosamine-4-sulfate-6-*O*-sulfotransferase; P-ORN, poly-DL-ornithine; NF, neurofilament; MAP2, microtubule-associated protein 2; PAPS, phosphoadenosine 5'-phosphosulfate; ELISA, enzyme–linked immunosorbent assay; BSA, bovine serum albumin; APS, aminopropyl-triethoxysilane; ME, mercaptoethanol; HPLC, high performance liquid chromatography; DAB, 3, 3'-diaminobenzidine; PTN, pleiotrophin; P7, postnatal day 7; E 16.5, embryonic day 16.5; SS-DS, shark skin DS.

[2]ten Dam, G. B., van de Westerlo, E. M. A., Purushothaman, A., Bulten, H., Sweep, F. C. G. J., Massuger, L., Sugahara, K., and van Kuppevelt, T. H., submitted.

FIGURE LEGENDS

Fig. 1. **Characterization of the substrate specificity of the single chain variable fragment antibody GD3G7.** The reactivity of the antibody GD3G7 with various GAG species was analyzed by ELISA, in which authentic commercial GAGs [CS-A, CS-B, CS-C, CS-D, CS-E, and heparin (Hep)] and the DS preparation from shark skin (SS-DS), were included. Biotinylated GAGs (2 μg each) were individually immobilized to wells of a streptavidin-coated plastic plate, and processed for incubation with the primary antibody GD3G7 (diluted 10-fold). Bound antibodies were visualized by subsequent incubation with mouse anti-VSV antibody P5D4 followed by alkaline phosphatase-linked goat anti-mouse Ig (G+M) (diluted 5,000-fold). Enzymatic activity was measured using *p*-nitrophenylphosphate as a substrate at 415 nm. Negative controls received no primary antibody. Bars represent the mean ± SD (n= 3).

Fig. 2. Anion-exchange HPLC and gel filtration chromatographic analyses of the reaction products prepared using zebrafish GalNAc4S-6ST as an enzyme source and nitrous acid-treated CS-B as the sulfate acceptor. An aliquot of ^{35}S-labeled CS-B produced by zebrafish GalNAc4S-6ST was digested with chondroitinase ABC (A and D), AC-I (B and E) or B (C and F). One half of each digest was analyzed by gel filtration on a Superdex Peptide column (A-C). The other half was analyzed by anion-exchange HPLC on an amine-bound silica PA-03 column using a linear NaH_2PO_4 gradient, as indicated by dashed lines, over a 60-min period (D-F). The vertical lines indicate the elution positions of standard even-numbered oligosaccharides derived from porcine skin DS (34). The numbered bars (A-C): 1, hexasaccharides; 2, tetrasaccharides; 3, disaccharides (D-F). The numbered arrows (D-F) indicate the elution positions of the authentic unsaturated disaccharides. 1, ΔDi-0S (ΔO); 2, ΔDi-6S (ΔC); 3, ΔDi-4S (ΔA); 4, ΔDi-diS_D (ΔD); 5, ΔDi-diS_E (ΔE); 6, ΔDi-triS (ΔT).

Fig. 3. **Reactivity of antibody GD3G7 towards CS-B treated with GalNAc 4S-6ST.** CS-B treated with zebrafish GalNAc4S-6ST was used as an inhibitor of the binding of GD3G7 to immobilized CS-E. Each GAG at 0.1 (white bars), 0.5 (grey bars) and 1.0 (black bars) μg was tested by performing an inhibitory ELISA. GalNAc4S-6ST transferred sulfate to the 6-*O*-position of GalNAc4S residues adjacent to IdoUA in CS-B and eventually generated iE units. Note that GalNAc4S-6ST-treated CS-B and also CS-H inhibited the binding of GD3G7 to CS-E, while native CS-B or CS-D did not bind GD3G7. Values were obtained from the average of two separate experiments.

Fig. 4. ***In situ* hybridization for *GalNAc4S-6ST* in the mouse brain during postnatal development.** Consecutive sagittal sections of the brain from P7 (A), P14 (B), P21 (C and E) and 7W (D) mice were hybridized with ^{35}S-labeled antisense (A-D) or sense (E) cRNA probes for GalNAc4S-6ST, and exposed to an X-ray film for 1 week. No labeling was observed in the respective neighboring sections hybridized with the sense probe (E and data not shown). The GalNAc4S-6ST transcript showed a widespread expression in the developing brain except at P7, when strong expression was observed in the external granule cell layer (arrowhead) in the cerebellum. The expression in the granule cell layer switched to the internal region and appeared to decrease slightly with development. Strong expression of GalNAc4S-6ST was also observed in the olfactory bulb, hippocampus, cerebral cortex and striatum of the developing brain. OB, olfactory bulb; Cx, cerebral cortex; Hi, hippocampus; Cb, cerebellum; St, striatum. Scale bar, 5mm.

Fig. 5. **Immunohistochemical localization of GD3G7 epitope in mouse brain.** Consecutive sagittal sections from P7 mouse brain were stained using the single chain variable fragment anti-CS antibody GD3G7 as described under "Experimental Procedures". Immunoreactivity to GD3G7 was observed in the P7 cerebellum, hippocampus and olfactory bulb. The staining completely disappeared on treatment of the tissue sections with chondroitinase ABC. Scale bars, 2 mm. For abbreviations, OB, Cx, Hi and Cb, see the legend to Fig. 4.

Fig. 6. **Effect of a single chain variable fragment antibody GD3G7 on the neurite growth of hippocampal neurons in culture.** Antibody GD3G7 was added to the culture medium at two different concentrations (10 μg/ml and 100 μg/ml) 2 h prior to the seeding of hippocampal cells from E16.5 mice on a substratum coated with CS-E. After a 24-h culture, the cells were immunostained with anti-MAP2 and anti-NF antibodies. Representative images of the cell morphology obtained in the absence (A) or presence (B) of 100 μg/ml GD3G7 are shown. C, effects of GD3G7 on neurite growth were evaluated by measuring the total length of the neurites per cell. An irrelevant scFv antibody MPB49V (100 μg/ml) was run as a negative control. The values represent the mean ± SD of those obtained from

two independent experiments in triplicate. **, $0.001<p<0.01$, significant difference from the values obtained in the experiments without exogenous antibody.

Fig. 7. **Determination of the minimum size of CS-E oligosaccharides for the recognition by GD3G7.** A, Even-numbered oligosaccharide fractions (0.5 μg) derived from CS-E of squid cartilage were tested by ELISA as inhibitors of the reactivity of GD3G7 with immobilized CS-E. Note that the decasaccharide fraction was the smallest fraction to show significant inhibitory activity, although the octasaccharide fraction seemed to react slightly with GD3G7 compared with the hexasaccharide fraction. B, different doses of CS-E octa and decasaccharide fractions (0, 0.5, 1 and 2 μg) were tested by ELISA as an inhibitor of the reactivity of GD3G7 with immobilized CS-E. Note that GD3G7 reacted preferentially with the decasaccharide fraction from CS-E. Values were obtained from the average of two separate experiments.

Fig. 8. **Effect of CS-E oligosaccharides on the immunohistochemical staining of GD3G7 epitope in mouse brain.** CS-E deca- and octasaccharides (1 nmol) were tested as inhibitors of the staining of GD3G7 in P7 mouse brain. Note that pre-incubation of GD3G7 with decasaccharides abolished the staining of the mouse brain sections while the staining was still observed after using octasaccharides as inhibitors.

Fig. 9. **Reactivity of structurally defined CS-E octa- and decasaccharides with GD3G7.** Four structurally defined decasaccharide fractions and one octasaccharide fraction prepared from CS-E were used as inhibitors of the reactivity of GD3G7 with immobilized CS-E. 0.01, 0.05 and 0.1 nmol of each decasaccharide fraction and 0.1 nmol of octasaccharide fraction were tested. Note that all four decasaccharide fractions but not the octasaccharide showed inhibitory activity. The values represent the mean ±SD of those obtained from two independent experiments.

Table I. **Reactivity of the CS-E oligosaccharide fractions to the single chain antibody GD3G7**

Fractions[a]	Recognition by GD3G7[b]	Component structures[c]
VIIIs	+	E-E-E-E-E (80%) E-E-E-E-A (20%)
VIIIo	+	E-E-E-E-C (86%) E-E-E-E-A (9%) E-E-E-E-E (3%) E-E-E-A-A (2%)
VIIIq	+	E-E-E-E-A (96%) E-E-E-E-C (4%)
VIIIm	+	C-E-E-E-A (35%) E-E-E-A-A (58%)
IXs	_	E-E-E-E (90-92%) E-E-E-A (6%) E-C-E-E (1-2%) A-E-E-E (1-2%)

[a] Reference 41.

[b] Plus (+) and minus (-) indicate positive and negative inhibitory activity, respectively, against the binding of GD3G7 to immobilized CS-E in ELISA as described in the legend to Fig. 9.

[c]E, A and C stand for GlcUA-GalNAc(4S, 6S), GlcUA-GalNAc(4S), and GlcUA-GalNAc(6S), respectively.

Figure 1

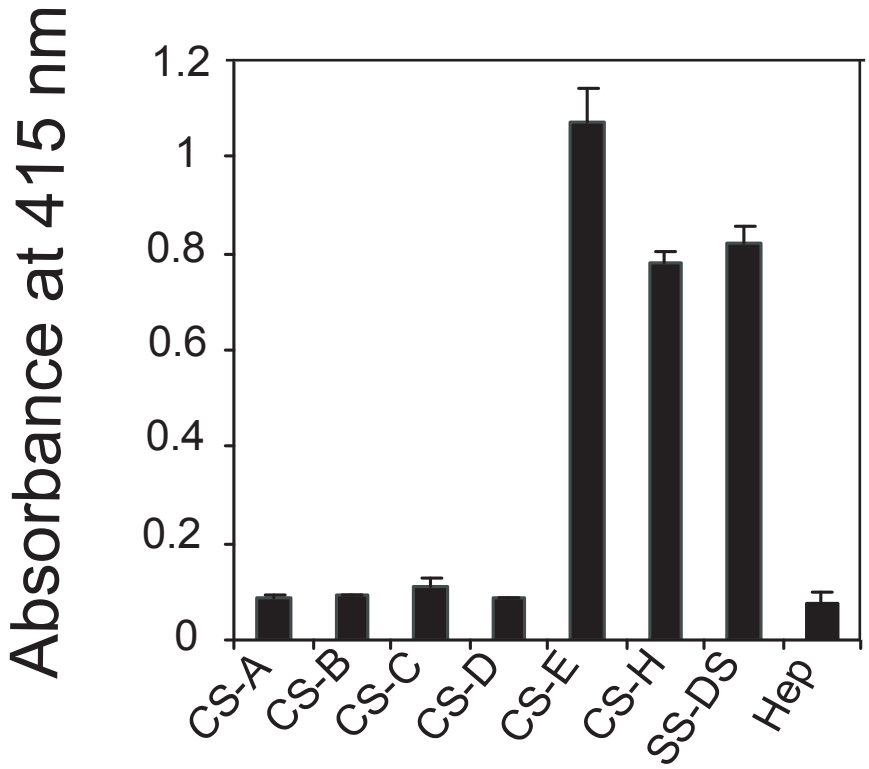
Absorbance at 415 nm
1.2
1
0.8
0.6
0.4
0.2
0
CS-A
CS-B
CS-C
CS-D
CS-E
CS-H
SS-DS
Hep

Figure 2

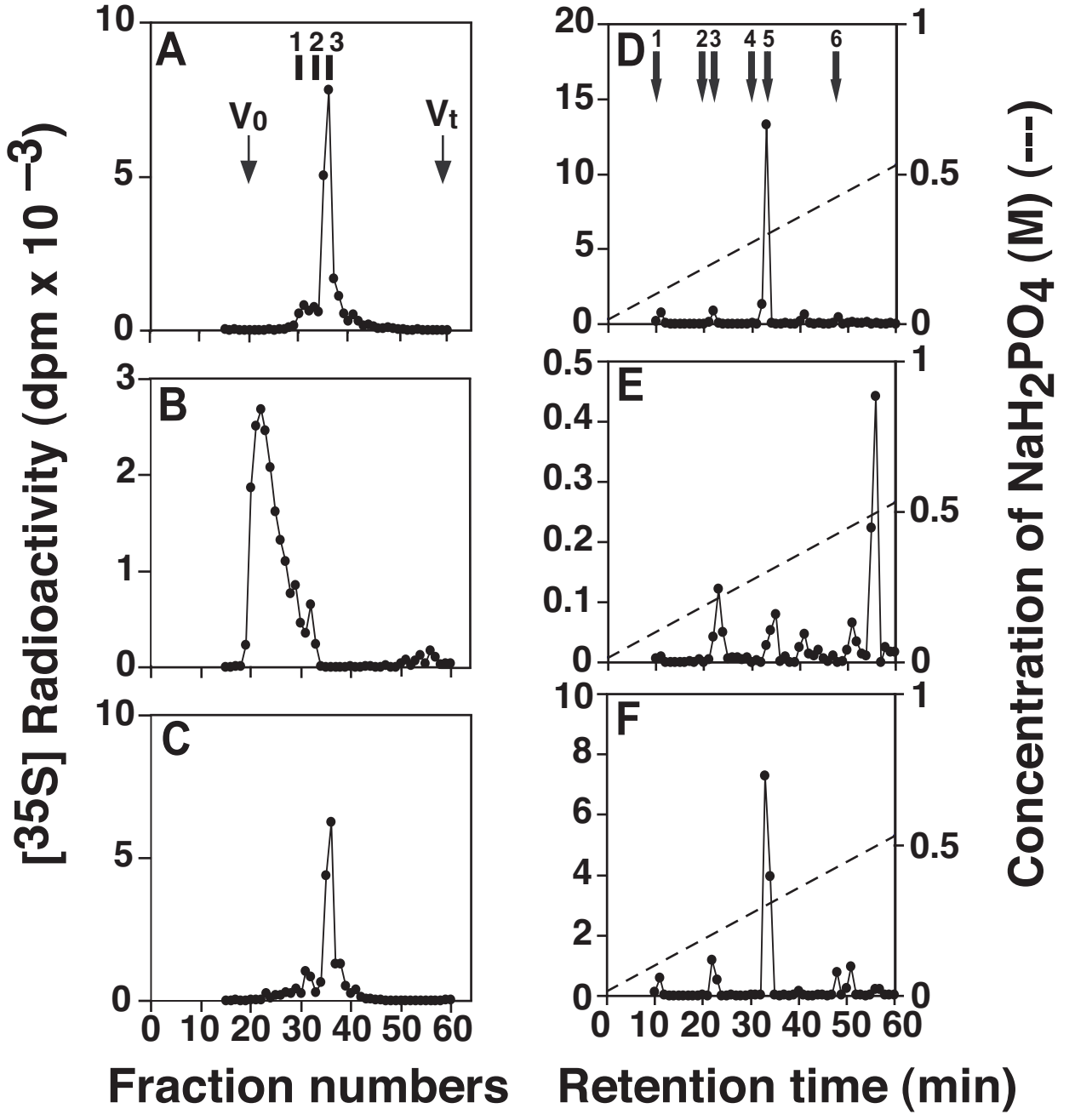
A
B
C
D
E
F
1 2 3
V_0
V_t
1
2 3
4 5
6
[35S] Radioactivity (dpm x 10 −3)
Concentration of NaH_2PO_4 (M) (---)
Fraction numbers
Retention time (min)

Figure 3

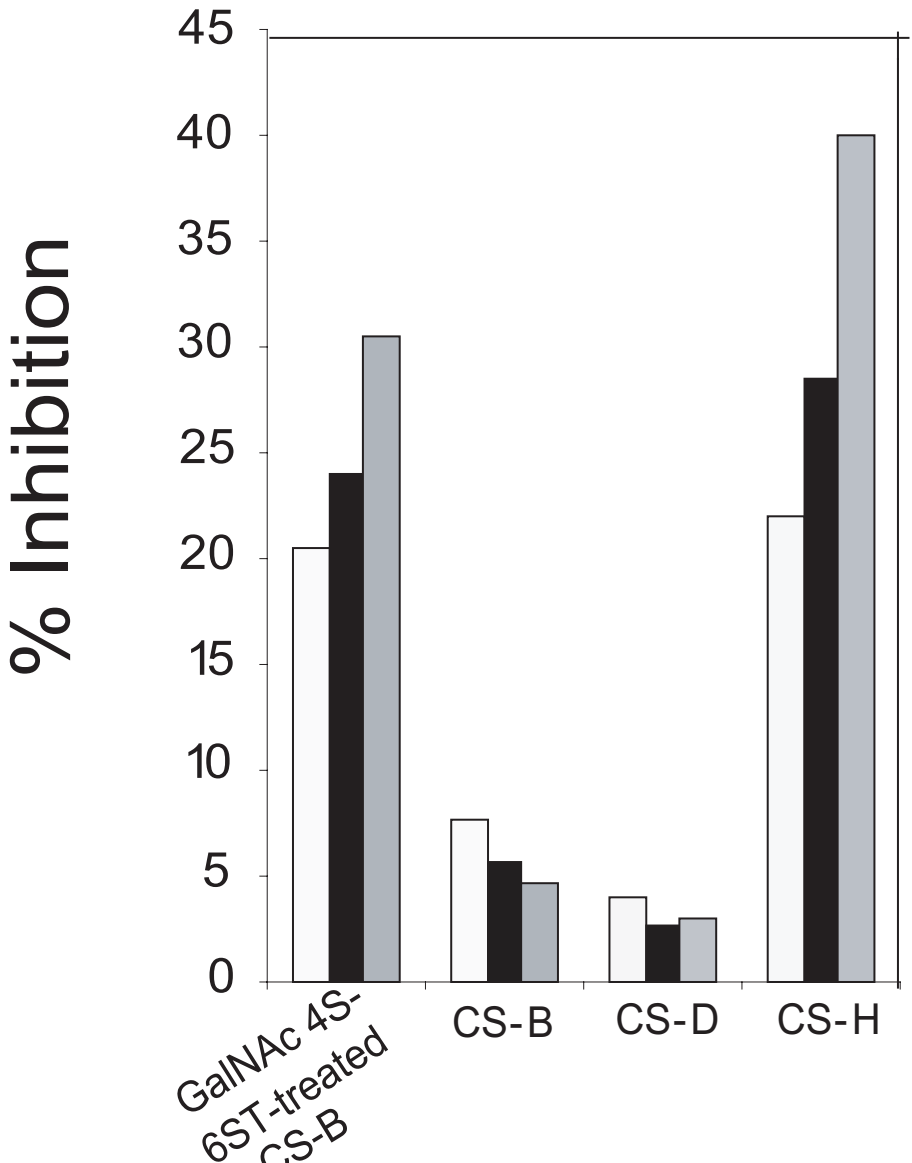
% Inhibition
45
40
35
30
25
20
15
10
5
0
GalNAc 4S-6ST-treated CS-B
CS-B
CS-D
CS-H

Figure 4

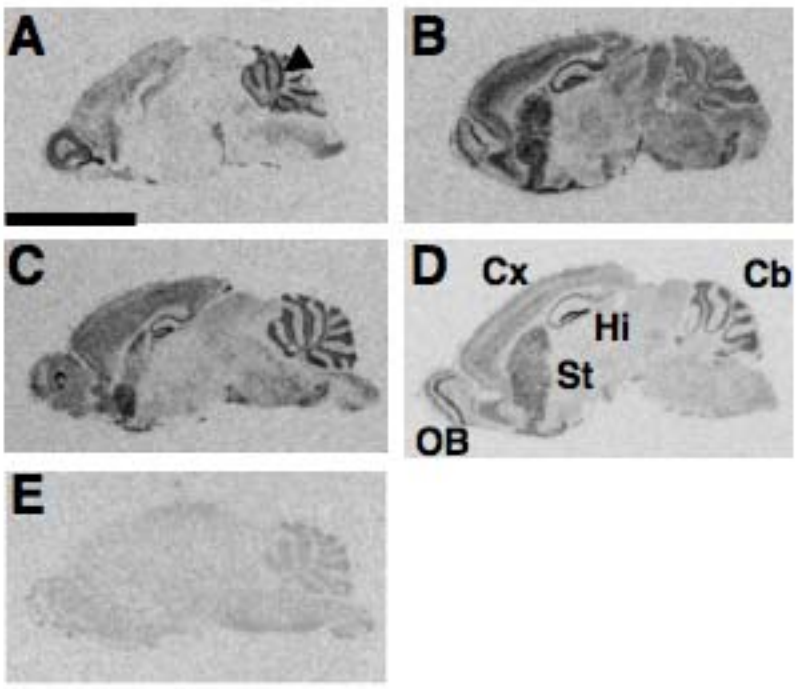

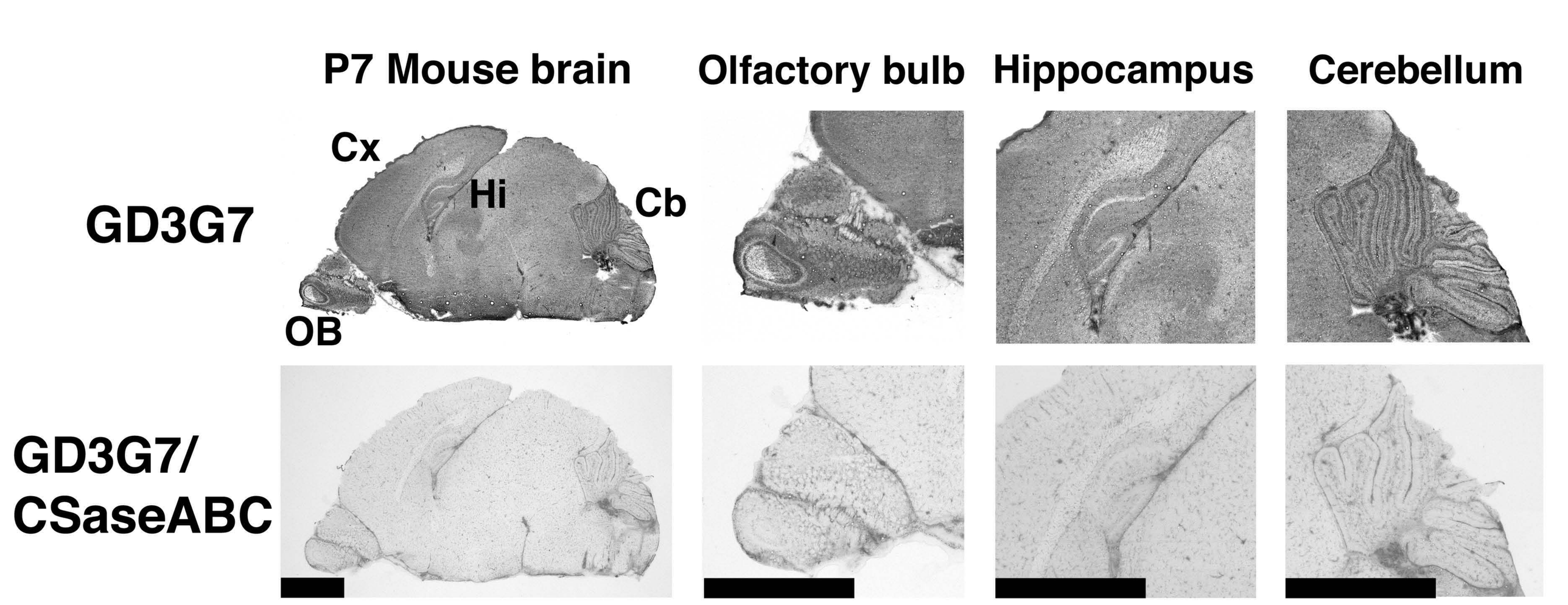
P7 Mouse brain
Olfactory bulb
Hippocampus
Cerebellum
GD3G7
Cx
Hi
Cb
OB
GD3G7/
CSaseABC

Figure 5

Figure 6

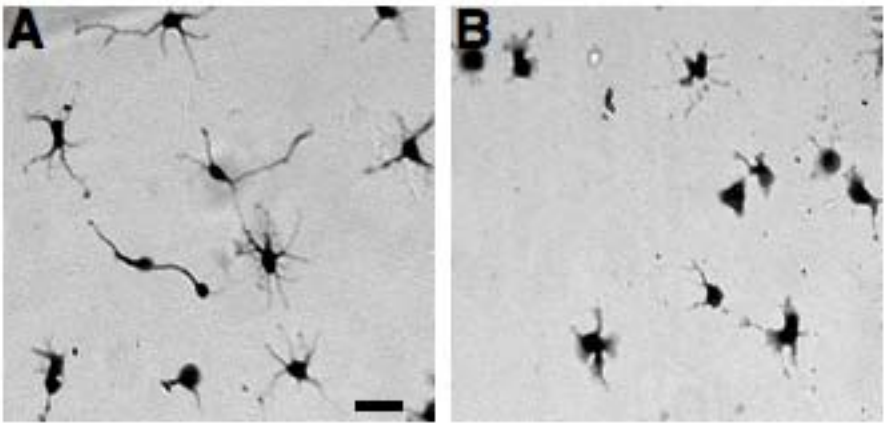
A
B

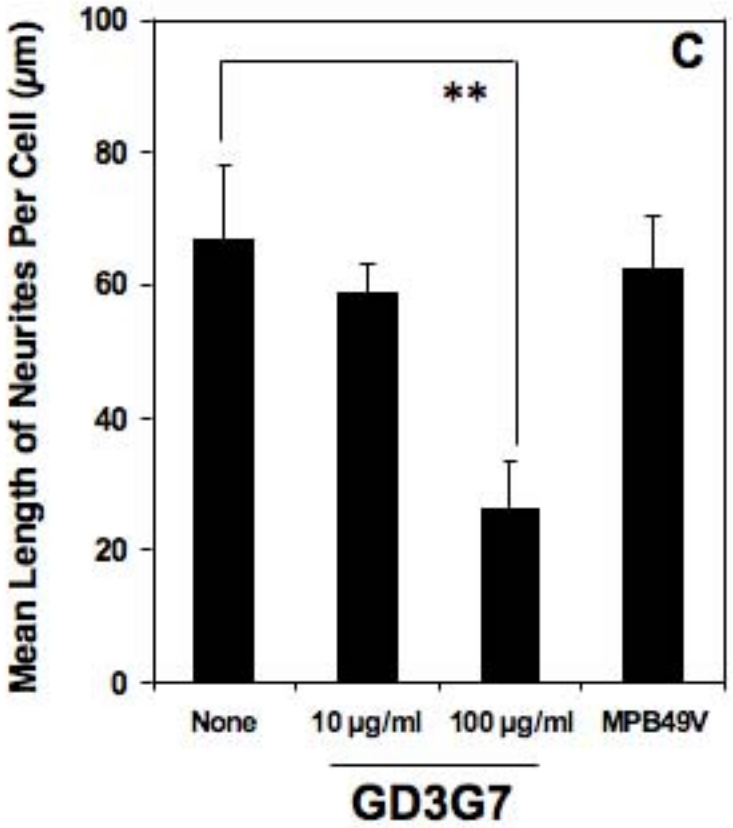
C
**
Mean Length of Neurites Per Cell (μm)
100
80
60
40
20
0
None
10 μg/ml
100 μg/ml
MPB49V
GD3G7

Figure 7

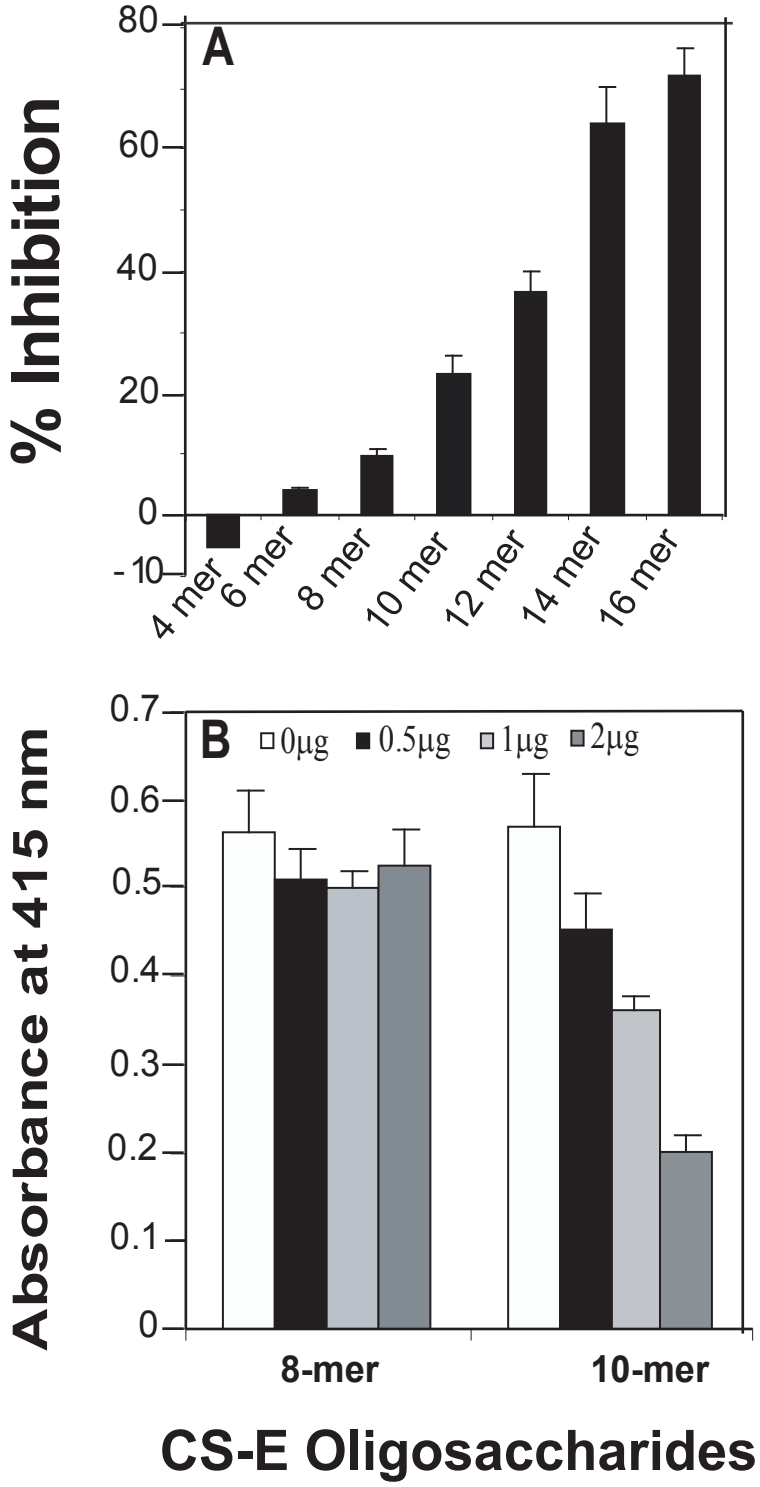
A
% Inhibition
80
60
40
20
0
-10
4 mer
6 mer
8 mer
10 mer
12 mer
14 mer
16 mer
B
0µg
0.5µg
1µg
2µg
Absorbance at 415 nm
0.7
0.6
0.5
0.4
0.3
0.2
0.1
0
8-mer
10-mer
CS-E Oligosaccharides

Figure 8

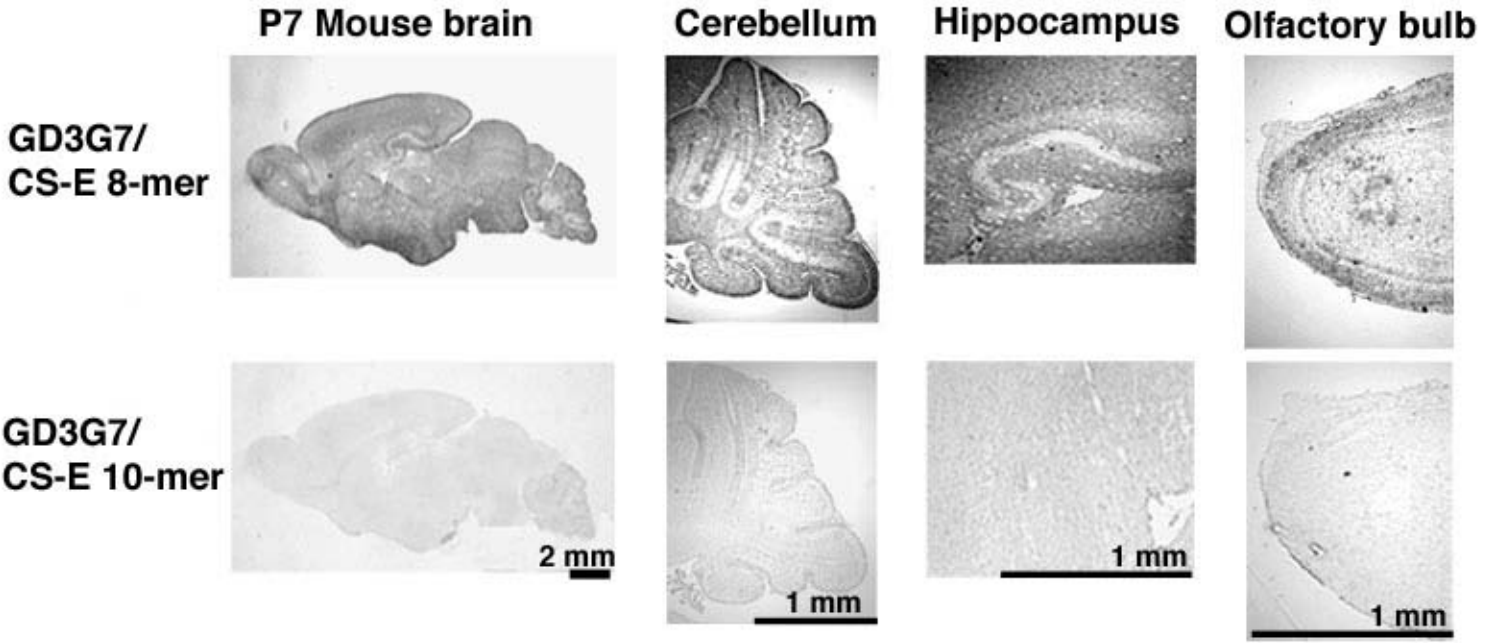
P7 Mouse brain
Cerebellum
Hippocampus
Olfactory bulb
GD3G7/
CS-E 8-mer
GD3G7/
CS-E 10-mer
2 mm
1 mm
1 mm
1 mm

Figure 9

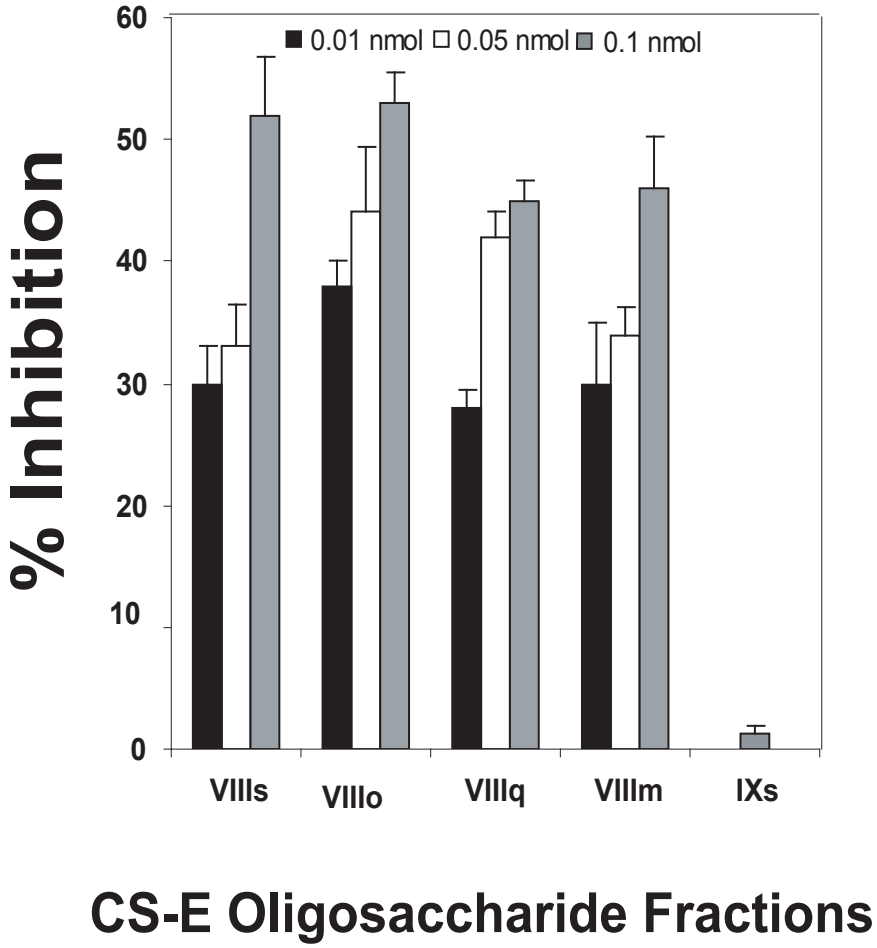
60
50
40
30
20
10
0
% Inhibition
0.01 nmol
0.05 nmol
0.1 nmol
VIIIs
VIIIo
VIIIq
VIIIm
IXs
CS-E Oligosaccharide Fractions

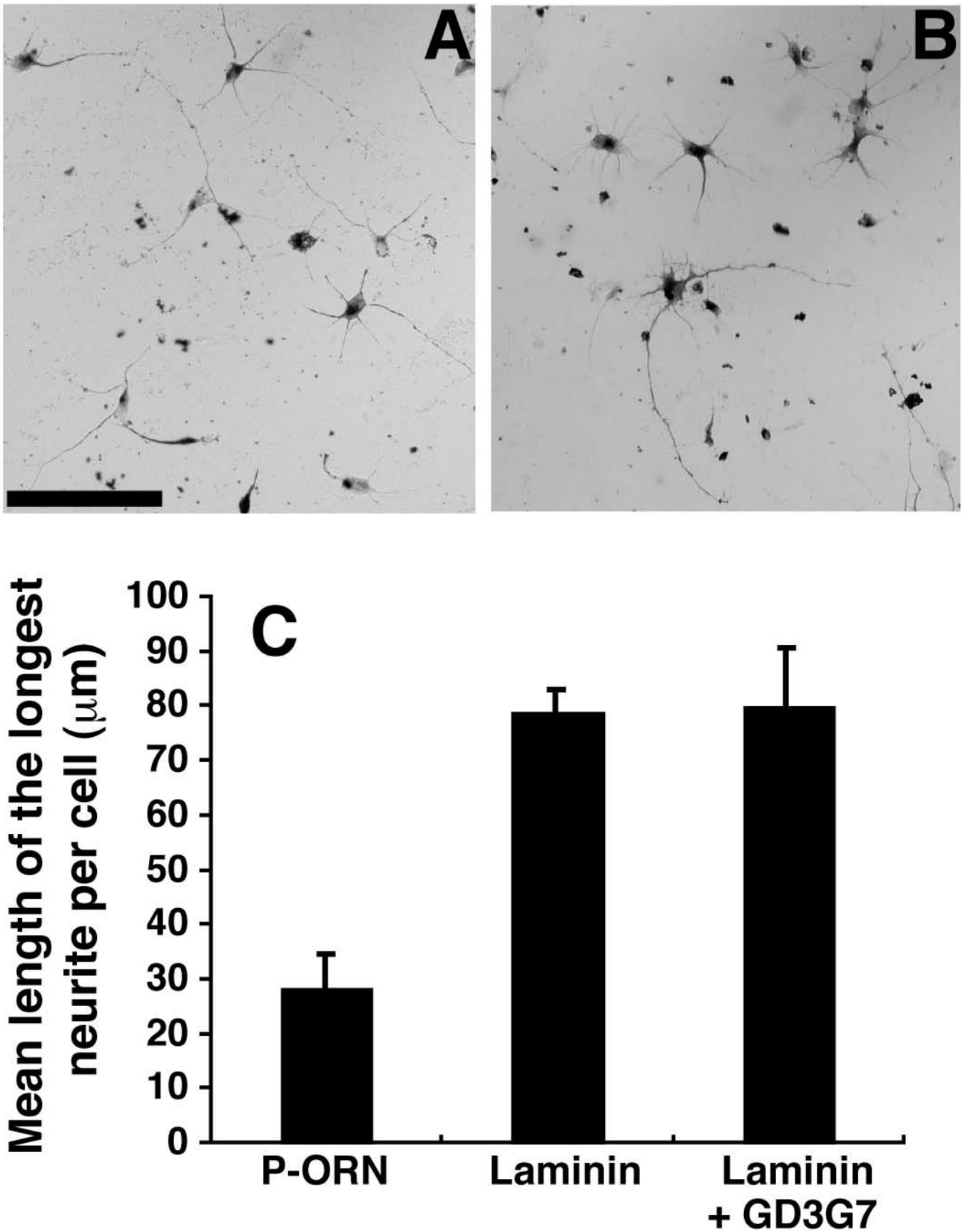
A
B
C
Mean length of the longest neurite per cell (μm)
100
90
80
70
60
50
40
30
20
10
0
P-ORN
Laminin
Laminin + GD3G7

Figure S1

Figure S1. **Effects of antibody GD3G7 on the neurite outgrowth of hippocampal neurons cultured on the laminin substrate.** Antibody GD3G7 (100 μg/ml) was added to the culture medium 2 h prior to the seeding of hippocampal neurons from E16.5 mice on a substratum coated with mouse laminin (10 μg/cm^2) according to Hikino *et al.* (16). After a 24-h culture, the cells were immunostained with anti-MAP2 and anti-NF antibodies. Representative images of the cell morphology obtained in the absence (A) or presence (B) of GD3G7 are shown. *C*, 100 randomly selected individual neurons were used to measure the mean length of the longest neurite under each set of conditions. Hippocampal neurons cultured on the poly-DL-ornithine (P-ORN) substratum were used as a negative control. Note that GD3G7 showed no inhibition against the neurite outgrowth induced by laminin. The values represent the mean ± SD of those obtained from two independent experiments in triplicate. The scale bar, 100 μm.